Simulation and Validation of a Precise 2RC Model of Lithium-Ion cell Incorporating Wire-bond Losses

Kunwar Aditya
IEEE Senior Member and Assistant Professor,
Department of Electrical Engineering
Indian Institute of Technology Jodhpur
Jodhpur- 342037, India
kunwar.aditya@iitj.ac.in

2023 International Conference on Control, Communication and Computing (ICCC) | 979-8-3503-3412-8/23/$31.00 ©2023 IEEE | DOI: 10.1109/ICCC57789.2023.10165007

***Abstract* — Li-ion cell is a popular electrochemistry for energy storage devices in electric vehicles and portable electronics. This is mainly due to their relatively high energy-density and power-density compared to other types of battery chemistry. In a battery pack, several li-ion cells are interconnected in a series-parallel fashion to meet the current and voltage demands of the load. Interconnecting wires or wire-bonds add parasitic resistance to the current path, contributing to power loss. Therefore, it is essential to include wire-bond losses in the battery model to get an accurate prediction of battery performance. In this paper, the authors have developed a 2RC model of li-ion cells, taking into account the wire-bond losses. Simulation was performed in MATLAB Simulink and the simulated results were verified with hardware results obtained using a li-ion battery cycler.**

Keywords—Li-Ion Modelling, Electrical Equivalent Circuit Model, 2RC Model, Electric Vehicles, Energy Storage.

I. INTRODUCTION

Lithium-ion cells have become the unanimous choice for energy storage devices for electric vehicles (EVs) and portable electronics [1], [2]. This is due to their superior features over other battery chemistries, such as a long shelf life, high charge-discharge cycles, low shelf-discharge rate, high power and energy density, high specific power and energy density, and low-memory effect [3]-[5]. The specifications of a lithium-ion cell, such as terminal voltage and capacity, depend on the type of material used in the cell. Therefore, selecting an appropriate chemistry is vital to meet the required specifications of the application [6]. For example, nickel-manganese-cobalt (NMC) chemistry, widely used in EV applications, has an operating voltage range of 3.0-4.2V/cell and a nominal capacity of 150-220Wh/kg [7], [8]. Since a single cell cannot meet the energy requirements of an EV, several such cells are connected in series/parallel configurations to form a battery pack. However, rather than arranging all the cells and making a single big battery, OEMs use multiple smaller batteries called modules to make the final battery pack, as shown in Fig. 1.

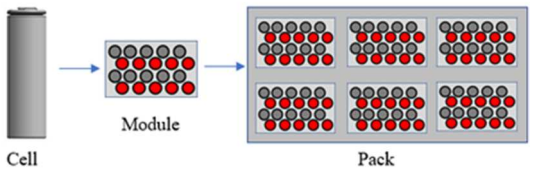

Fig. 1. Cell, module and battery pack illustration.

Cells are connected together using a wire-bonding process. The wire-bonding technique has been in use since the 1970s in the power electronics and microelectronics industry. It was adopted by Tesla Motors as a replacement for the commonly used spot-welding method to manufacture their battery pack [9]. Wire bonding allows cells to be connected from one side, so the rest of the cell body is free for cooling. Wire-bonds also act as a fusible link separating the cell from the pack in case of unfortunate events, therefore improving the safety and reliability of the overall system [10]. Aluminium wires of 400 µm are the most typical material used for the wire-bonding process, considering a fusing current of ~20A. For higher current ratings, two or more wire-bonds per joint can be used. Fig. 2 shows an illustration of wire-bond connecting cells from the top side to the busbars of the battery pack.

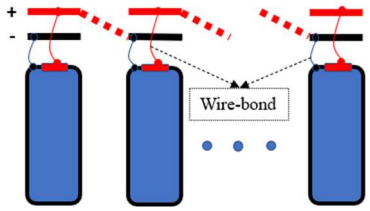

Fig. 2. Illustration of wire-bonds connecting cells to busbars of the pack.

State-of-charge (SOC) estimation is crucial for the power distribution strategy of EVs, predicting driving range, and controlling the overcharging and overdischarging of lithium-ion cells [11], [12]. For precise SOC estimation, an accurate battery model is required [13]. Wire-bonds resistance adds to the resistance of the lithium-ion cell and, therefore, must be modeled to get an accurate estimate of the SOC of the battery.

In the literature, a wide variety of cell models have been presented, which can be broadly categorized into Electrochemical models, Mathematical models, and Equivalent Circuit models (ECMs) [14], [15]. Among these, ECMs are very useful for electrical engineers as they are simple to understand, can be used in circuit simulators, and require less computational burden to solve. ECMs mainly include: Thevenin equivalent model; first, second, and third-order RC models; linear electric model; and impedance-based model. The 2RC model can capture the accurate dynamic behaviors of a lithium-ion battery. It can also accurately model the hysteresis effect and polarization effect in a lithium-ion cell, and it is simple to use. Fig. 3 shows the 2RC ECM of a lithium-ion cell.

979-8-3503-3412-8/23/$31.00 ©2023

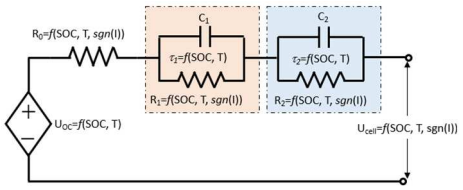

Fig. 3. 2RC equivalent circuit model of Li-Ion cell.

In Fig. 3, U_{oc} is open circuit voltage (OCV) of the cell; R_0 is equivalent series resistance (ESR) or Ohmic resistance or internal resistance of the cell; RC pairs (R_1, C_1, R_2, C_2) are diffusion resistances and capacitances; τ_1 and τ_2 are RC time constants; and U_{cell} is the terminal voltage. R_0 is used to characterize the instantaneous response of the cell voltage, whereas RC pairs are used to characterize the transient response of the cell voltage due to charge-transfer and diffusion processes [16]. All these parameters are non-linear functions of SOC and temperature (T). For more accuracy, one may be tempted to use three or more RC pairs. However, the 2RC model has proven to be a good compromise between model accuracy and simulation convergence time [17], therefore, it has been used in this paper.

In the next section, the proposed electrical model of lithium-ion cell considering wire-bond resistance is explained.

II. Li-Ion Cell Modelling

Fig. 4, shows the high-level model of Li-Ion cell created in MATLAB-Simulink.

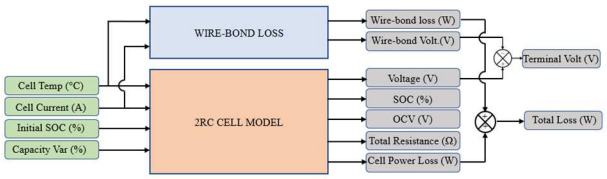

Fig. 4. High-level view of Li-Ion 2RC cell model with the wire-bond loss block.

Input and output parameters of the cell model is shown in Table I. This cell model can be connected in series and parallel to emulate a battery pack.

TABLE I. Input and Out Variables of Li-Ion Cell Model

Input	Output
Cell Current (A)	Terminal Voltage (V)
Cell Temperature (°C)	OCV (V)
Initial SOC (%)	Total resistance (Ω)
Capacity Variation (%)	SOC (%)
	Total losses (W)

Inside 2RC Cell Model Block: The 2RC model block consists of following parts: Coulomb counting and Coulomb to SOC conversion; Losses calculation; Lookup tables for parameters: R_0, R_1, R_2, τ_1 and τ_2 and OCV; and a subsystem to calculate terminal voltage and total resistance. Major subsystems have been explained below:

A. Coulomb counting and coulomb to SOC conversion

Estimating SOC via integral equation is called coulomb counting. SOC is related to cell current via equation (1).

$$SOC(t) = SOC(0) - \frac{1}{Q}\int_0^t \eta.i(\tau)d\tau \quad (1)$$

In Equation (1), cell current is positive during discharge and negative during charging process; η is cell coulombic efficiency (≤1); Q is the cell capacity in coulombs. Integrating the current over time gives Q in coulombs. To obtain it in Ah, it is divided by 3600. Fig. 5 shows the Simulink implementation of coulomb counting and SOC conversion.

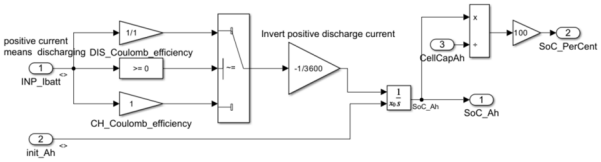

Fig. 5. Simulink implementation of coulomb counting and SOC calculation.

B. RC Network Calculation

The model makes heavy use of look-up tables to determine the model parameters. Data for look-up tables was obtained for SONY VTC6 cells. SONY VTC6 is rated for a nominal capacity of 3000 mAh at a nominal voltage of 3.7V. Its full-charge voltage is 4.2V, and it is capable of a maximum continuous discharge rate of 7c. The look-up tables are set to retrieve the value of R_0, R_1, R_2, τ_1, τ_2 and OCV from the SOC and Temperature of the cell as the input as shown in Table II. Fig. 6 shows the Simulink implementation of R_1 look up table as an example.

TABLE II. List of Look-up Tables Used in the Model

Look up table	Input of Look-up tables	Output
OCV	SOC in %	OCV in Volts
R_0 Charge		R_0 for charging current in Ohm
R_0 discharge		R_0 for discharging current in Ohm
R_1 Charge		R_1 for charging current in Ohm
R_1 discharge	Cell temperature in °C	R_1 for discharging current in Ohm
R_2 Charge		R_2 for charging current in Ohm
R_2 discharge		R_2 for discharging current in Ohm
τ_1		τ_1 constant time in s
τ_2		τ_2 constant time in s

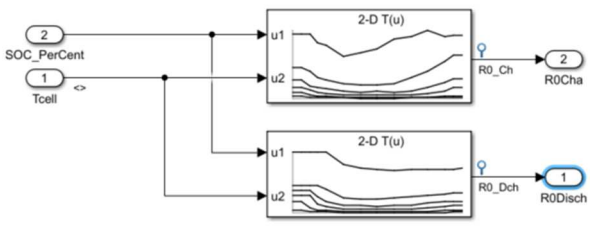

Fig. 6. Look-up table block for R_0(charging and discharging) calculation.

C. Terminal Voltage and Total Resistance

The RC voltage is resolved in continuous time in the form of a state space equation. To calculate the terminal voltage, current through the resistor is calculated. Considering a RC network as shown in Fig. 7, we can write:

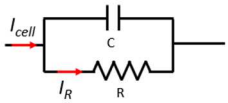

Fig. 7. Current flowing through Resistor in 2RC network.

$$\frac{di_R}{dt} = \frac{i_R}{\tau} - \frac{i_{cell}}{\tau} \tag{2}$$

$$i_R = \int \frac{di_R}{dt} dt \tag{3}$$

$$u_R = R \cdot i_R \tag{4}$$

Equation (2)-(4) were implemented in Simulink as shown in Fig. 8.

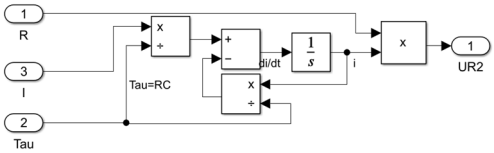

Fig. 8. Calculation of voltage drop across R_2 in Simulink.

Similarly, voltage drop across R and R_1 is calculated in Simulink and added together to get the total voltage drop. Finally, total voltage drop is subtracted from the OCV to get the terminal voltage.

D. Loss Calculation

The losses are calculated by taking the terminal voltage and subtracting the OCV to it. By multiplying this voltage to the cell current, the instantaneous losses are obtained. The formula is as follows:

$$P = |I_{cell}(U_{cell} - U_{OCV})| \tag{5}$$

Inside Wire-bond loss Block: The electrical resistance of the wire-bond is calculated with the properties of aluminium. It was hypothesized that the part of the wire-bond losses that were transferred to the cell was equal to the wire-bond losses minus what was dissipated by radiation. Energy that is not transferred to the cell increases the temperature of the wire-bond. Fig. 9 shows the wire-bond loss calculation implemented in Simulink.

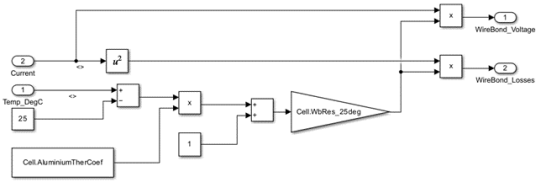

Fig. 9. Simulink model for integrating wire-bond losses in the Li-Ion cell

III. Model Verification

Fig. 10 shows the hardware setup to obtain current, temperature and voltage from SONY VTC6 cell. In Fig. 10, cycler is BTS-4000 high accuracy battery testing system from Neware; Li-Ion cell is US18650VTC6 3000mAh from SONY; thermal chamber was custom made from a local supplier which can be used to change the ambient temperature of the Li-Ion cell as well as to monitor and log the temperature of the cell in real time. Fig. 11 and Fig. 12 compares the experimental data with the simulation model data.

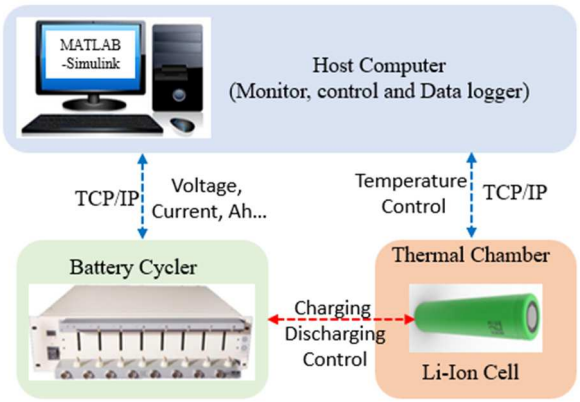

Fig. 10. Block diagram of battery test bench.

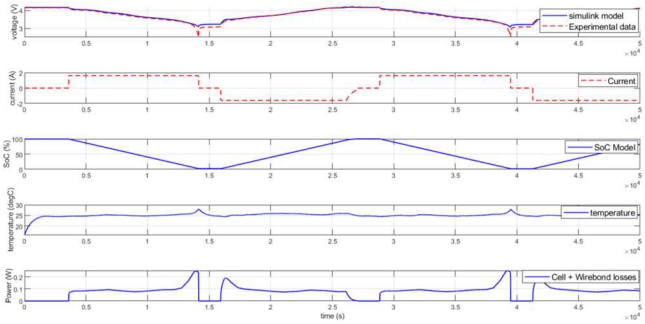

Fig. 11. Comparison of simulation model and experimental results for ambient temp of 25 °C.

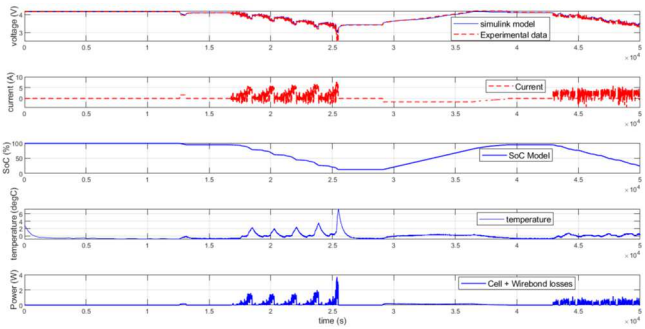

Fig. 12. Comparison of simulation model and experimental results for ambient temp of 0°C.

In Fig. 11 and Fig. 12, the 'blue' traces are from the real-time simulation model, and the 'red dotted' traces are from the experimental test bench. It should be noted that for simulation and experiment, the current will be the same, therefore, simulation results for the cell current have not been plotted. The cell is simulated with a discrete timestep. Therefore, to avoid false errors during transients, a correction is set by filtering with a sliding window to avoid false error calculations. It can also be observed that the calculated losses correspond to

an experimental increase in temperature, which is good behaviour. The error is below 2% except for SoC below 10%.

IV. Conclusions

An accurate battery model is imperative for an accurate estimate of the SOC of the battery. Loss in wire-bonds interconnecting lithium-ion cells affects the battery performance. Wire-bond resistance adds to the internal resistance of the cell, and therefore, it must be included in the battery model. In this paper, a lithium-ion 2RC model was created in the MATLAB Simulink environment, considering the wire-bond losses. Simulation was performed in the MATLAB Simulink, and simulated results were verified with hardware results obtained using a lithium-ion battery cycler. The model presented in this paper shows results very close to reality with an error below 2% if the SoC is above 10%. If the model needs to be more precise, new look-up tables can be loaded. In future work, the authors intend to use the cell model proposed in this paper to model an entire battery pack of an electric vehicle.

References

[1] Zhu, Q. Ouyang, Y. Wan and Z. Wang, "Remaining Useful Life Prediction of Lithium-Ion Batteries: A Hybrid Approach of Grey-Markov Chain Model and Improved Gaussian Process," in *IEEE Journal of Emerging and Selected Topics in Power Electronics, 2022*.

[2] H. Chun, K. Yoon, J. Kim and S. Han, "Improving aging identifiability of lithium-ion batteries using deep reinforcement learning," in *IEEE Trans. on Transportation Electrification*, 2022.

[3] X. Sun *et al*., "State of Power Capability Prediction of Lithium-Ion Battery from the Perspective of Electrochemical Mechanisms Considering Temperature Effect," in *IEEE Trans. on Transportation Electrification*, 2022.

[4] X. Tang, T. Jia, X. Hu, Y. Huang, Z. Deng and H. Pu, "Naturalistic Data-Driven Predictive Energy Management for Plug-In Hybrid Electric Vehicles," in *IEEE Trans. on Transportation Electrification*, vol. 7, no. 2, pp. 497-508, June 2021.

[5] M. Shehab El Din, A. A. Hussein and M. F. Abdel-Hafez, "Improved Battery SOC Estimation Accuracy Using a Modified UKF With an Adaptive Cell Model Under Real EV Operating Conditions," in *IEEE Transactions on Transportation Electrification*, vol. 4, no. 2, pp. 408-417, June 2018.

[6] W. Vermeer, G. R. Chandra Mouli and P. Bauer, "A Comprehensive Review on the Characteristics and Modeling of Lithium-Ion Battery Aging," in *IEEE Transactions on Transportation Electrification*, vol. 8, no. 2, pp. 2205-2232, June 2022

[7] M. A. Hannan, M. M. Hoque, A. Hussain, Y. Yusof and P. J. Ker, "State-of-the-Art and Energy Management System of Lithium-Ion Batteries in Electric Vehicle Applications: Issues and Recommendations," in *IEEE Access*, vol. 6, pp. 19362-19378, 2018.

[8] X. Chen, W. Shen, T. T. Vo, Z. Cao and A. Kapoor, "An overview of lithium-ion batteries for electric vehicles," *2012 10th International Power & Energy Conference (IPEC)*, 2012, pp. 230-235.

[9] C. Rouff, “A closer look at wire bonding,” in Charged Electric Vehicles Magazine, Aprl 2016.

[10] J. Straubel, D. Lyons *et al*., "Battery pack and method for protecting batteries," United States Patent US7671565B2, 2006.

[11] H. He, R. Xiong, X. Zhang, F. Sun and J. Fan, "State-of-Charge Estimation of the Lithium-Ion Battery Using an Adaptive Extended Kalman Filter Based on an Improved Thevenin Model," in *IEEE Transactions on Vehicular Technology*, vol. 60, no. 4, pp. 1461-1469, May 2011.

[12] M. S. Hossain Lipu, M. A. Hannan, A. Hussain, M. H. Saad, A. Ayob and M. N. Uddin, "Extreme Learning Machine Model for State-of-Charge Estimation of Lithium-Ion Battery Using Gravitational Search Algorithm," in *IEEE Transactions on Industry Applications*, vol. 55, no. 4, pp. 4225-4234, July-Aug. 2019.

[13] C. Vishnu and A. Saleem, "Adaptive Integral Correction-Based State of Charge Estimation Strategy for Lithium-Ion Cells," in *IEEE Access*, vol. 10, pp. 69499-69510, 2022.

[14] R. Rao, S. Vrudhula and D. N. Rakhmatov, "Battery modeling for energy aware system design," in *Computer*, vol. 36, no. 12, pp. 77-87, Dec. 2003.

[15] M. Chen and G. A. Rincon-Mora, "Accurate electrical battery model capable of predicting runtime and I-V performance," in *IEEE Transactions on Energy Conversion*, vol. 21, no. 2, pp. 504-511, June 2006.

[16] S. Amir, M. Gulzar, M. O. Tarar, I. H. Naqvi, N. A. Zaffar and M. G. Pecht, "Dynamic Equivalent Circuit Model to Estimate State-of-Health of Lithium-Ion Batteries," in *IEEE Access*, vol. 10, pp. 18279-18288, 2022.

[17] C. Liao, H. Li and L. Wang, "A dynamic equivalent circuit model of LiFePO4 cathode material for lithium ion batteries on hybrid electric vehicles," *2009 IEEE Vehicle Power and Propulsion Conference*, 2009, pp. 1662-1665.